ADIPOCYTE
2018, VOL. 7, NO. 3, 156–165
https://doi.org/10.1080/21623945.2018.1493900

Taylor & Francis
Taylor & Francis Group

RESEARCH PAPER

3D MicroCT spatial and temporal characterization of thoracic aorta perivascular adipose tissue and plaque volumes in the ApoE-/- mouse model

Erin Faight[a], Kostas Verdelis[b], Joseph M. Ahearn[a], and Kelly J. Shields [a]

[a]Lupus Center of Excellence, Autoimmunity Institute, Department of Medicine, Allegheny Health Network, Pittsburgh, PA, USA; [b]Division of Endodontics at the Department of Restorative Dentistry and Comprehensive Care and the Department of Oral Biology, University of Pittsburgh, Pittsburgh, PA, USA

ABSTRACT

Perivascular adipose tissue (PVAT) influences vascular function and pathology. We present a protocol using micro-computed tomography (microCT), a novel imaging technique typically used for hard biological tissue, to characterize the temporal and spatial development of aorta PVAT and luminal plaque soft tissue. Apolipoprotein E deficient (ApoE) and C57Bl/6J (control) mice were fed a high fat western diet up to 30 weeks. 3D microCT reconstructions were used to quantify: 1) vascular wall volume, a surrogate measure of remodeling, was greater in ApoE, 2) aorta PVAT volume was reduced in ApoE, 3) plaque volumes increased over time in ApoE, 4) plaque development co-localized with luminal ostia, origins of branching arteries, which traveled through areas of greatest PVAT volume, 5) qualitatively, the same arteries showed evidence of increased tortuosity in ApoE. This study reflects the potential of microCT analyses to assess vascular wall, PVAT and arterial trajectory modifications in relevant animal models.

Abbreviations: PVAT: perivascular adipose tissue; ApoE: apolipoprotein E deficient mouse strain; Control: C57Bl/6J mouse strain; PTA: 0.3% phosphotungstic acid; microCT: micro-computed tomography; CV: cardiovascular; CVD: cardiovascular disease; IQR: interquartile range; PPARγ: peroxisome proliferator activated receptor – gamma; VV: vasa vasorum; 3D: three dimensional

ARTICLE HISTORY
Received 8 May 2018
Accepted 21 June 2018

KEYWORDS
3D microCT; perivascular adipose tissue; plaque imaging; Apolipoprotein E deficient mouse

Introduction

Heart disease is the leading cause of death for both men and women in the United States[1] There is no doubt that excessive adipose tissue contributes to poor cardiovascular (CV) health and adverse CV outcomes[2-4] Perivascular adipose tissue (PVAT) is a small, visceral adipose depot in close proximity to blood vessels with no adventitial fascial boundary, which has a direct influence on vascular function, inflammation and vascular pathology including cardiovascular disease (CVD) progression[5-8]

Conventional theory suggests the development of luminal plaques and progression to clinically diagnosed CVD is an 'inside-out' response initiated at the intima due to a disruption of the endothelial cell layer ultimately leading to an inflammatory response orchestrated by circulating molecules and cells[5] We have previously suggested an alternative to this process by implicating the PVAT surrounding the blood vessel supporting an 'outside-in' approach. Using a common mouse model of atherosclerosis we found increased vascular stiffness, a marker of vascular wall remodeling, along with complement protein deposition, a part of the innate immune system and a marker of inflammation, on the elastin within the extracellular matrix of the vascular wall and surrounding PVAT. We hypothesized that the complement deposition detrimentally affects the mechanical integrity of the elastin causing the increased vascular stiffness[8,9] We translated this work to determine if there were differences in PVAT volumes in a cohort of women with systemic lupus erythematosus (SLE), a population that tends to develop CVD at a much younger age, by developing a protocol utilizing clinical computed tomography (CT) scans. We found greater volumes of descending thoracic aorta PVAT associated with CVD measures[10]

Indeed there is intense clinical interest to develop quantitative measures implicated in CVD progression or CV events, which has led some to focus on the PVAT and, in particular, various measures derived from clinical CT scans including thresholding techniques and attenuation indices[10-12] The goal of this study was to develop a technical protocol beginning with

CONTACT Kelly J. Shields kelly.shields@ahn.org Allegheny Health Network, Allegheny General Hospital, 320 E North Avenue, 8th Floor South Tower, Pittsburgh, PA 15212, USA

appropriate soft tissue labeling through to imaging with high resolution 3D micro-computed tomography (microCT) in order to dramatically improve the ability to evaluate animal models of cardiovascular disease. This novel imaging technique is typically used for hard biological tissue,[13–15] however, we are using the technique to characterize the temporal and spatial development of 1) aorta vascular wall volume – a surrogate measure of vascular remodeling, 2) aorta PVAT volume and 3) luminal plaque volume in a robust atherosclerotic mouse model[16-20]

Materials and methods

Animals

Five week old atherosclerosis-prone apolipoprotein deficient (-/-) (ApoE, n = 8) mice with a B6 background and standard C57BL/J (control, n = 8) mice were acquired from Jackson Laboratories, Bar Harbor, ME, USA. The mice were housed within the animal facility of Allegheny-Singer Research Institute and allowed to acclimate for 2 weeks. At 7 weeks of age, both ApoE and control were started on a high fat, Western diet (TestDiet, St. Louis, MO) (32.5% Fat, 48.1% Carbohydrates, 19.4% Protein) *ad libitum*. Mice were sacrificed at 12 weeks (ApoE: n = 2; control: n = 2), 22 weeks (ApoE: n = 2; control: n = 2), and 30 weeks (ApoE: n = 4; control: n = 4). All experimental protocols were approved by the Institutional Animal Care and Use Committee.

MicroCT

Thoracic aortas were harvested after euthanasia from each group as previously described[8] Briefly, the descending thoracic aorta was flushed with saline to remove residual blood and the aortic arch and celiac trunk were used as anatomical proximal and distal landmarks, respectively. Immediately following excision, the aorta was washed in phosphate buffered saline (PBS) and fixed in formalin for 24–48 hours on a rocking platform at 4°C. After rinsing the aortas 3 times with PBS the aortas were placed into 0.3% phosphotungstic acid (PTA) for 72–96 hours on a rocking platform at 4°C. PTA is regularly used in standard histology techniques including hematoxylin staining protocols and as a negative stain for transmission electron microscopy. In this context, PTA is used as a contrast agent due to differential absorption properties in soft tissue extracellular matrix constituents such as collagen and fibrin[21]

Each thoracic aorta was individually imaged in a customized holder with 70% EtOH medium using a Skyscan 1172 (Bruker-Skyscan, Contich, Belgium) microCT system with a 3 μm voxel resolution and the following conditions: 40 kVp, 250 uA, 300 ms exposure, rotation step 0.40 degrees, frame averaging 15. Three-dimensional (3D) volumes of the aortas were reconstructed from the lateral views using NRECON (Bruker-Skyscan) software with a beam hardening correction set at 25% and a cone-beam reconstruction mode.

The imaged aortas were processed and analyzed separately. Using CT-Analyzer (CTAn) software (Bruker-Skyscan), user-defined regions of interest (ROI) were created by tracing the contour of: i) aorta vascular wall (outside of the tunica adventitia), ii) aorta lumen, and iii) perivascular adipose tissue. For the ApoE aortas, a separate ROI was traced for the plaques. Care was also taken to create ROIs for large veins and their corresponding lumens (e.g. inferior vena cava) for exclusion in the overall PVAT volume. All ROIs were then processed as separate datasets to obtain volumes of interest (VOI: i) aorta vascular wall, ii) aorta PVAT, and iii) plaque). For the post-scan analysis, we used direct 3D measurements that have been well documented in characterizing bone microarchitecture such as volume thickness for the aorta wall[22,23] Two evaluators (KS and KV) independently quantified the volume of a random subset of aortas for the reproducibility analysis. Excellent intra- and inter-reader reproducibility for the volume (intraclass correlation coefficient (ICC) 0.99 and 0.90, respectively) was demonstrated for the designated microCT parameters and post-scan tracing protocol. Only one reader (KS) completed the volume defining ROIs for this study.

To generate 3D renderings, images were imported into a workstation operating in an open VMS-environment and processed by Scanco (Scanco Medical, Brutisselen, Switzerland) 3D morphometry software.

Histology

After completion of the microCT scans and analysis, the aortas were cryopreserved by perfusing the lumen with OCT freezing medium, embedding the aorta vertically in a block of the same OCT, and snap freezing in liquid nitrogen. Using a cryostat (Leica CM3050, Wetzlar, Germany), 5μm serial sections were cut at −20°C, mounted on superfrost plus™-lined glass slides and stored at −20°C until use. Standard histology techniques were used in conjunction with a Masson's Trichrome kit. (All histology supplies were purchased through Newcomer Supply, Middleton, WI)

Statistics

Non-parametric comparisons between the groups were performed using a Kruskal-Wallis test (within strain

comparisons at 12 vs 22 vs 30 weeks) or Wilcoxon rank-sum test (between strain comparisons at each time point). Post hoc analyses were performed using a Bonferroni correction with adjusted p-value. Non-parametric covariates were expressed as median and interquartile range (IQR = 25^{th}-75^{th}%). All statistical analyses were performed using Stata/IC 12.1 (StatCorp, LP, College Station, TX).

Results

Thoracic aorta samples were segmented by utilizing the various soft tissue density differences to create 2D regions of interest (ROIs) of the: **1)** aorta vascular wall, **2)** aorta PVAT, and **3)** plaque (ApoE only) (Figure 1A-C). The 2D ROIs were then reconstructed to form 3D volumes for qualitative and quantitative analyses.(Figure 2) The control aorta (Figure 2A,B) shows a uniform vascular wall thickness (red), a lumen with no plaque formation, periodic ostia with the coinciding arterial branches traversing through the surrounding, uniform PVAT (gray). The ApoE aorta (Figure 2C,D) shows a non-uniform vascular wall thickness (red), a lumen with extensive plaque formation (yellow) co-localized at the ostia with coinciding arterial branches revealing a marked degree of tortuosity as they traverse through the surrounding, non-uniform PVAT. We are also able to note the qualitative difference in relative transparency of the PVAT between the control (Figure 2B) and ApoE (Figure 2D) despite using identical thresholding conditions for the both reconstructions.

Aorta vascular wall volume was greater in apoe mice at 30 weeks

The extent of vascular wall remodeling can be evaluated through changes in aorta vascular wall thickness and is typically assessed using serial 2D histology images. In this study, we utilized the 3D capabilities of microCT to quantify overall aorta vascular wall volume (Table 1) and subsequently evaluate the vascular wall volume as a function of vascular wall thickness ranges. (Figure 3A-E)

Overall, we did not find any statistically significant differences in aorta vascular wall volume between time points in either strain ($p > 0.1$, ApoE or control) or between ApoE and control at 12 or 22 weeks.(Table 1) However, at 30 weeks, the aorta vascular wall volume in ApoE (median(IQR)): 1.55(1.26–1.90) mm^3) was significantly greater when compared to control (1.13 (1.01–1.14) mm^3, $p = 0.02$).(Table 1)

The aorta vascular wall thickness histograms show increasing aorta vascular wall volumes within higher thickness ranges for both strains with age. (Figure 3A-B) Additionally, the ApoE strain demonstrates a trend towards greater vascular wall volumes within the higher thickness ranges at each time point when compared to the control strain and significantly greater at 30 weeks ($p = 0.02$).(Figure 3C-E)

Aorta PVAT volume was greater in control mice at 30 weeks

We found no statistically significant differences between time points for the ApoE aorta PVAT volume. However, we demonstrated a trend of

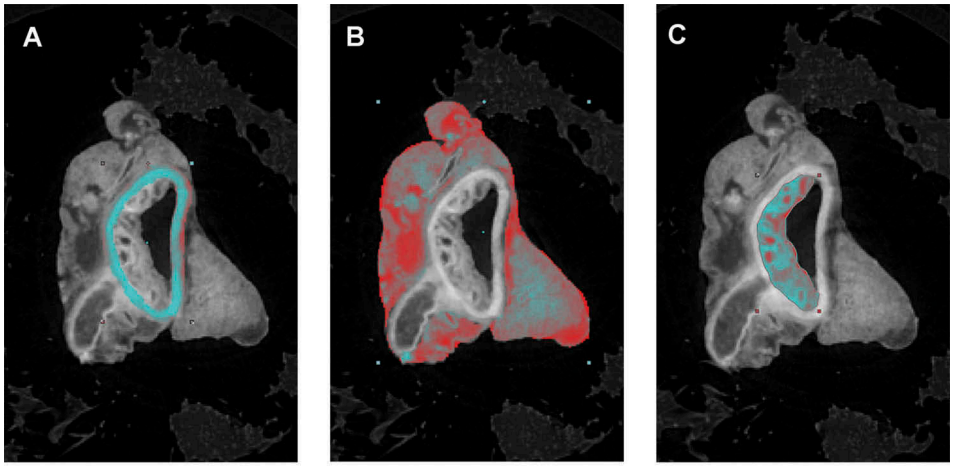

Figure 1. Post-scan processing representative tracings of 2D regions of interest (ROIs): A) aorta vascular wall, B) aorta PVAT, C) plaque (in ApoE only).

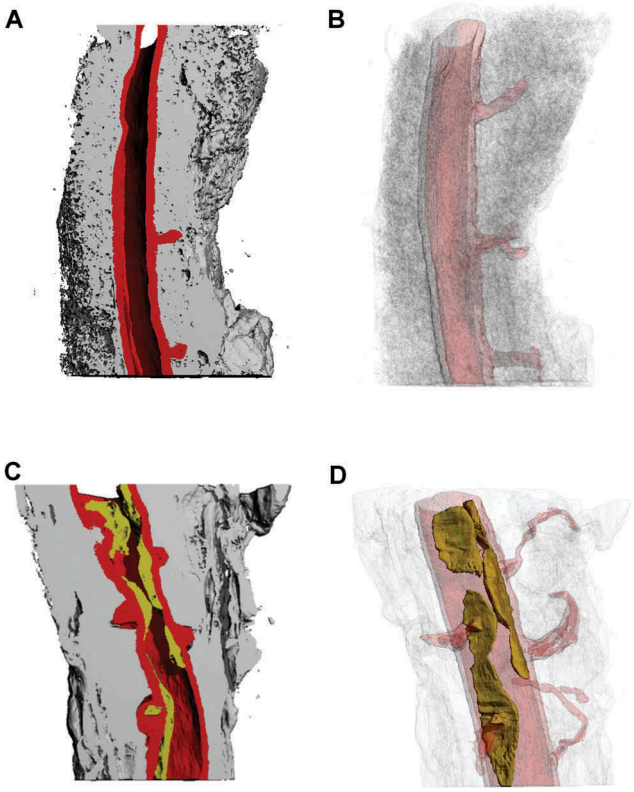

Figure 2. 3D microCT renderings using both solid and various levels of transparency to reveal aorta lumen, vascular wall, and surrounding PVAT of the descending thoracic aorta at 30 weeks old. Control: A) Solid, longitudinal cut plane revealing aorta lumen, vascular wall, and surrounding PVAT, B) Relative transparency of aorta lumen, vascular wall, and surrounding PVAT. ApoE: C) Solid, longitudinal cut plane revealing aorta lumen, vascular wall, and surrounding PVAT, D) Relative transparency of aorta lumen, vascular wall, and surrounding PVAT. The same 3D reconstruction thresholding conditions were used for all solid and relative transparent models..

increasing aorta PVAT volume with age in the control ($p = 0.077$).(Table 1 and Figure 4) We found no differences in aorta PVAT volume at 12 or 22 weeks between ApoE and control. Surprisingly, however, at 30 weeks the ApoE had significantly less aorta PVAT volume when compared to the control ($p = 0.02$). (Table 1 and Figure 4)

Plaque volume increased with age in apoe mice

We isolated plaque volumes in ApoE mice along the length of the thoracic aorta using microCT segmentation. We did not detect any plaque formation at 12 weeks. Plaque volumes were quantified at 22 weeks (0.181(0.163–0.199) mm^3) and were significantly less when compared to the plaque volumes at 30 weeks (0.516(0.316–0.882) mm^3, $p = 0.049$). (Table 1)

Co-localization of plaque formation: branching arteries and aorta PVAT leaflets

One of the greatest advantages of using microCT to analyze soft tissue is the ability to serially progress through the tissue in its entirety. In particular, we were able to detect and quantify plaque volumes and their spatial relation with the surrounding PVAT, as well as to identify various anatomic markers along the length of the lumen such as intercostal ostia. PTA incubation also allowed us to view the small arterial branches originating from the aorta ostia (e.g. posterior intercostal arteries, mediastinal and esophageal branches) and travelling through the surrounding PVAT.(Figure 2)

Even at 30 weeks on a high fat diet, the control maintained a clear aorta lumen with no vascular wall disruptions at the intima except for the ostia. The arterial branches in the control strain remained open with no occlusions as they progressed through the PVAT. (Figure 5A-C, G-I) At 30 weeks, the ApoE had well-defined plaques surrounding the arterial ostia, which spread through the lumen both circumferentially and distally. (Figure 5D-F, J-L) In comparison to the control arterial branches stemming from the ostia, the ApoE arterial branches narrowed and were at times occluded, suggesting development of plaques in the smaller arterial branches.

MicroCT and histological differences between strains: PVAT architecture

Using the serial images of the microCT, we are also able to note between-strain differences in the architecture of

Table 1. Quantitative microCT parameters. Comparison of MicroCT segmented aorta vascular wall, PVAT, and plaque volumes in the Control and ApoE strains at 12, 22 and 30 weeks. (median(IQR)) * $p = 0.02$ and $^{\dagger}p < 0.05$.

	Control			ApoE (-/-)		
	12 weeks	22 weeks	30 weeks	12 weeks	22 weeks	30 weeks
Aorta Vascular Wall Volume (mm^3)	0.437 (0.41–0.46)	1.21 (1.1–1.3)	1.13 (1.0–1.1)*	0.544 (0.54–0.55)	1.42 (1.4–1.4)	1.55 (1.3–1.9)*
Aorta PVAT Volume (mm^3)	2.68 (2.4–3.0)	11.0 (9.6–13)	16.1 (15–17)*	2.46 (2.2–2.7)	5.90 (5.3–6.5)	6.69 (5. 9–7.2)*
Total Plaque Volume (mm^3)	N/A	N/A	N/A	No plaque formation	0.181 (0.16–0.20)†	0.516 (0.32–0.88)†

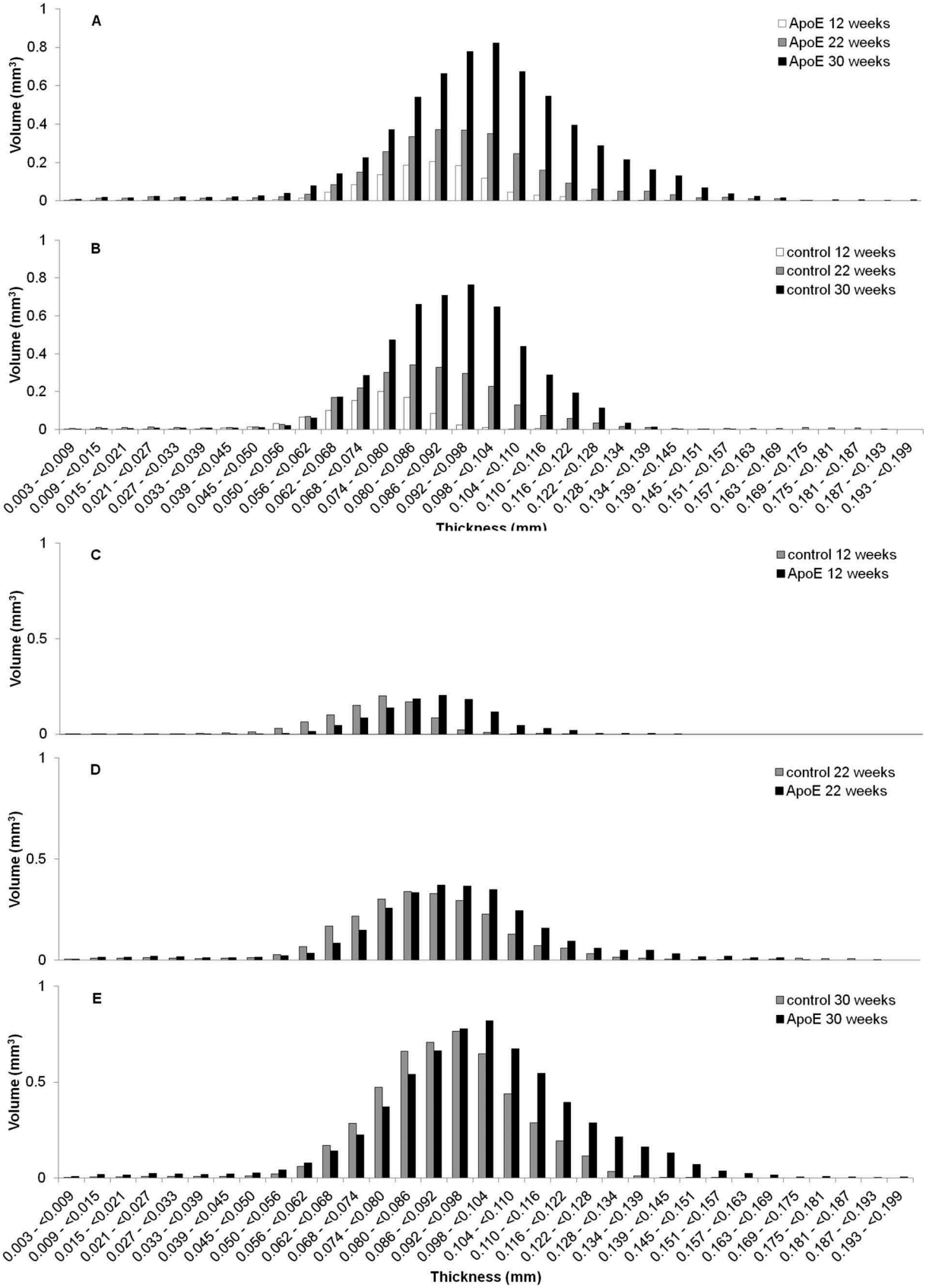

Figure 3. Distribution vascular wall thicknesses throughout the length of descending thoracic aorta. The distributions presented are pooled from all the specimens within either the ApoE or control groups. Within strain, between time points: A) ApoE and B) Control (CTL) at 12, 22, and 30 weeks. Between strain, at each time point: C) 12 weeks, D) 22 weeks, E) 30 weeks (*,p = 0.02).

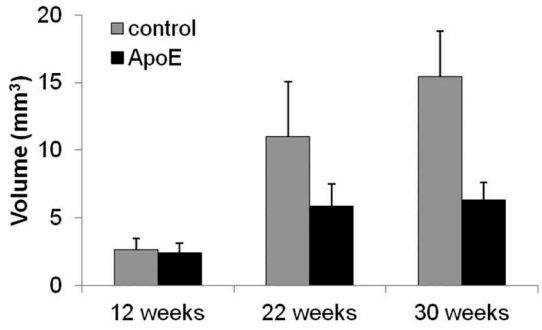

Figure 4. Overall aorta PVAT volume for the control and ApoE groups over time. When comparing within strain, the control trends towards a steadily increasing aorta PVAT volume with age (p = 0.08, shaded bars only). When comparing between strains, the ApoE (6.69(5.89–7.17) mm^3) had significantly less aorta PVAT when compared to control (16.1(14.8–16.8) mm^3) at 30 weeks (*,p = 0.02).

the aorta PVAT. The control animals had a well-defined cross-sectional area with notable fascial lines surrounding the boundaries of PVAT that is separated into a distinct tri-leaflet pattern (Figure 5A-C, G,H), which we have previously observed through scanning electron microscopy,[8] while the PVAT in the ApoE was notably less well-defined (Figure 5C-E, J,K).

The serial images of the microCT allowed us to specify locations along the length of the aorta to section for a histological comparison. We purposefully selected sections along the length of the aorta that would allow us to visualize a cross-section of an arterial branch beginning at ostia within the aorta lumen, proceeding through the aorta vascular wall, and traversing through the surrounding PVAT.(Figure 5, control: H, I and ApoE: K, L) The representative Masson's Trichrome images revealed that the control aorta PVAT had more staining for cytoplasm within the PVAT tri-leaflets (Figure 5I, red), while the ApoE aorta PVAT had increased staining for extracellular collagen within the PVAT tri-leaflets (Figure 5L, blue) indicating a marked difference in extracellular matrix composition between strains with increased PVAT remodeling in the ApoE strain, which is also qualitatively represented in the microCT images (Figure 5H shows distinct adipocyte architecture in the PVAT leaflet, while Figure 5K shows a non-distinct, soft tissue morphology)

Discussion

We optimized soft tissue staining and microCT scanning, reconstruction and thresholding parameters to evaluate the vascular wall remodeling using changing vascular wall volume along with surrounding PVAT and plaque volume development in a mouse model of atherosclerosis. Surprisingly, we were also able to reveal co-localization of the plaque development with aorta ostia and also follow the paths of the branching arteries traversing through the surrounding PVAT along with

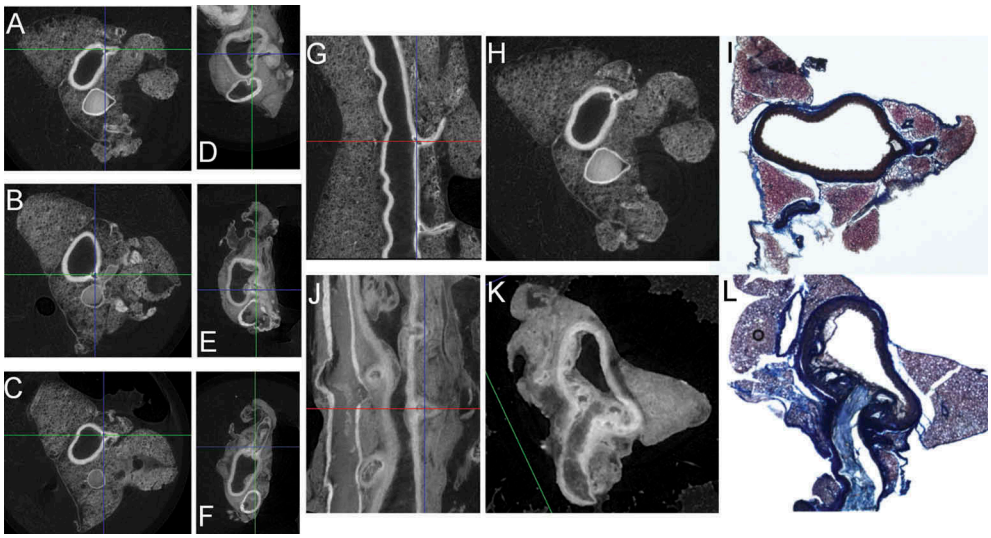

Figure 5. Serial MicroCT images through the descending thoracic aorta allow for unparalleled detail of the lumen, luminal ostia leading to arterial branches (e.g. intercostal arteries) through the vascular wall and traversing the surrounding PVAT along with visualizing the co-localization of plaque development with luminal ostia and PVAT leaflets. Representative microCT images of aorta branching and extending through the surrounding PVAT leaflets at 30 weeks: Transverse sections (proximal to distal) A-C) Control, D-F) ApoE; Coronal sections G) Control, J) ApoE. Based on the microCT scans, we can target different lengths of the aorta for histology. Luminal arterial ostia progressing through vascular wall and traversing surrounding PVAT: Control: H) MicroCT cross-section, I) Cryo-sectioned aorta stained with Masson's Trichrome at same level as (H); ApoE with plaque: K) MicroCT cross-section, L) Cryo-sectioned aorta stained with Masson's Trichrome at same level as (K).

revealing an increased level of tortuosity for branching arteries in the ApoE. This study demonstrates that microCT analysis coupled with standard histology techniques and appropriate murine models may provide a comprehensive evaluation of vascular pathology and the contribution of PVAT in various disease models.

Adipose tissue is capable of acting as an endocrine organ entering into either an anti- or pro-inflammatory state. Aorta PVAT is a small visceral adipose depot originally thought to only provide structural support for the aorta. Similar to other vasculature including the coronary and carotid arteries, there are no fascial boundaries separating the vascular wall from the surrounding PVAT supporting the hypothesis of unfettered localized, paracrine activity on the vascular walls. There is evidence that a shift from a normal biological adipose response towards an inflammatory response may elicit a strong, localized influence on vascular remodeling and CVD[24,25] Recent findings by Oyhama, et al, continue to support the idea of an 'inside-to-outside' pathway for the progression of CVD with the surrounding PVAT acting as a biological sensor of vascular dysfunction[26] In addition, Antonopoulos, et al, has also found evidence of vessel-derived inflammatory signals both inducing lipolysis and blocking angiogenesis in response to vascular disease progression[11] We have previously found evidence of extensive complement protein labeling within the surrounding aorta PVAT either halting at the external elastic lamina (B6-control) or progressing through the aorta vascular wall and attaching to the elastin (ApoE) suggesting an 'outside-in' phenomenon[8] The progression of vessel dysfunction to CVD is a multifaceted, complex interplay most likely combining aspects of both inside (vessel-derived) and outside (PVAT-derived) signaling and response mechanisms.

The studies reported here led to several observations. We observed that the ApoE had less PVAT volume. The ApoE strain does not have the metabolic issues, such as insulin resistance, commonly observed in murine models of obesity, but there are indications of altered adipocyte lipid uptake including triglycerides[27,28] This impaired lipid uptake has also been linked to peroxisome proliferator activated receptor – gamma (PPARγ), a master regulator of adipogenesis. Under hypertrophic conditions within adipose tissue, impaired adipogenesis may be, at least in part, responsible for an overall lack of visceral adipose and the much reduced aorta PVAT volume in the ApoE[28,29]

Second, we noted that the ApoE aorta PVAT had a high degree of collagen indicative of tissue fibrosis when compared to the control PVAT. Healthy adipose has an extracellular matrix that promotes function including the ability to expand and stimulate angiogenesis, while fibrosis has been linked to obese states and inflammation[30-32] Exacerbated adipose tissue inflammation may result from altered adipocyte metabolism, thus promoting increased adipose tissue fibrosis and acute, localized vascular wall inflammation[12]

More recently, methods have been developed using clinical CT scans have been used to assess the radiodensity differences within adipose tissue either through novel, post-scan thresholding techniques, a combination of positron-emission tomographic (PET)-CT, or through innovative development of a Fat Attenuation Index (FAI)[11,12,33,34] In general, adipose tissue is a heterogeneous mix of differing adipocytes, immune regulating cells, and extracellular matrix, which can be clearly demarcated using standard 2D histology and immunohistochemistry techniques. Within this study, the resolution of the microCT permitted us to qualitatively note differences in the PVAT tri-leaflet architectur[8] between the ApoE and control strain, including defining fascial boundaries within the PVAT and at the perimeter along with density differences in ApoE plaques. Qualitatively, given the same microCT reconstruction conditions, one can see that the control PVAT density appears to be different (Figure 2B) when compared to the ApoE PVAT (Figure 2D). With proper calibration standards and microCT parameters, a longitudinal, 3D microCT radiodensity analysis of appropriate CVD murine models could potentially determine if higher or lower density PVAT preferentially develops surrounding the vasculature or co-localizes with plaque development.

Third, along the length of the descending aorta in the ApoE, we found plaque development at periodic ostia corresponding to branching arteries. Paigen, et al, and Sloop, et al, found similar patterns at the ostia in ApoE mice and within human aortas, respectively[35,36] Most contend that points of arterial branching result in disrupted blood flow inherently altering the hemodynamic shear stresses experienced by the intimal layer. Endothelial cell dysfunction of the intimal layer leads to a localized inflammatory response and plaque development, which then exacerbates the altered blood flow and furthers vessel dysfunction and plaque formation[36,37] From the serial microCT images, we can clearly observe the branching arteries originating at luminal ostia and traveling through the PVAT. The PVAT provides mechanical support for the aorta and the branching aorta arteries. These branching arteries increase the vascular wall surface area exposed to the potential, acute inflammatory environment occurring in the surrounding PVAT. Langheinrich, et al, used microCT to assess the development of vasa vasorum (VV) along the length of the descending thoracic aorta with plaque development in

the ApoE/LDL(-/-). They found that the volume of arterial VV was associated with plaque formation and the arterial VV originate from intercostal arteries, which stem from the descending thoracic aorta[38] The adventitial inflammation cited by Langheinrich, et al, may also be due in part to a more extensive inflammatory environment within the surrounding PVAT where we previously found extensive complement labeling implicating an immune response[8] A part of the working hypothesis is that complement proteins covalently binding via the internal thioester to vascular wall structural proteins compromises the biomechanical integrity leading to increased vascular stiffness. We can visualize the increased tortuosity of the branching arteries, which may be due to both increased stiffness and a concomitant degradation of the structural integrity of the surrounding PVAT. Lastly, with evidence of plaque occluding the lumen of the small branching arteries, it is possible that the effects of acute inflammation occurring in the PVAT surrounding these smaller branching arteries may be more profound than elsewhere in the aorta due to the relative volume of PVAT to vascular wall thickness of these branching arteries.

It should be noted that a limiting factor in this study was the small number of samples; however, the quantitative method afforded by microCT allows for a better ascertainment of vascular wall, aorta PVAT and plaque volumes when compared to histological evaluation of limited serial tissue sections. We believe these initial data provide a solid foundation for future studies to extend our observations Additional studies utilizing microCT might be complemented by histologic and immunohistochemical analyses to determine molecular and cellular constituents of the vascular wall, plaque and aorta PVAT. Pairing such data with radiodensity measures of the tissue may also facilitate determination of adipose tissue and plaque quality, which may lead to novel targets for therapeutic intervention.

In conclusion, we have successfully developed a comprehensive protocol beginning with the soft tissue staining through the optimized microCT imaging and reconstructions in order to characterize vascular remodeling, PVAT and plaque volume co-localization, and potentially PVAT integrity along with arterial tortuosity. These efforts have demonstrated spatial co-localization of PVAT, plaque, and luminal ostia, suggesting potential causal relationships and the need for subsequent investigations utilizing this approach.

Acknowledgments

The authors wish to thank Dr. Michael J. Passineau for his editorial assistance and Rong Chong for her expertise in developing the 3D renderings.

Author Contributions

EF: Contributed to histology protocol development, histological analysis, review of manuscript.
KV: Contributed to microCT protocol development, critical review/revision of manuscript
JA: Contributed concept/design of experiments, critical review and revision of manuscript
KS: Contributed to concept/design of experiments, microCT and histology protocol development, microCT data analysis, statistical analysis, drafting/critical review and revision of manuscript

Disclosure of potential conflicts of interest

No potential conflicts of interest were disclosed.

Ethical Approval

All experimental protocols were approved by the Institutional Animal Care and Use Committee of the Allegheny Health Network Research Institute.

ORCID

Kelly J. Shields http://orcid.org/0000-0002-5699-7773

References

1. Benjamin EJ, Blaha MJ, Chiuve SE, Cushman M, Das SR, Deo R, De Ferranti SD, Floyd J, Fornage M, Gillespie C, et al. Heart disease and stroke statistics-2017 update: a report from the american heart association. Circulation. 2017 Mar 7;135(10):e146–e603. PubMed PMID: 28122885; PubMed Central PMCID: PMCPMC5408160.
2. Kannel WB. Lipids, diabetes, and coronary heart disease: insights from the Framingham Study. Am Heart J. 1985 Nov;110(5):1100–1107. PubMed PMID: 4061265; eng.
3. Hotamisligil GS. Inflammation and metabolic disorders [Research Support, N.I.H., Extramural Research Support, Non-U.S. Gov't Review]. Nature. 2006 Dec 14;444(7121):860–867. PubMed PMID: 17167474; eng.
4. Mongraw-Chaffin M, Foster MC, Anderson CAM, Burke GL, Haq N, Kalyani RR, Ouyang P, Sibley CT, Tracy R, Woodward M, et al. Metabolically healthy obesity, transition to metabolic syndrome, and cardiovascular risk. J Am Coll Cardiol. 2018 May 1;71(17):1857–1865. PubMed PMID: 29699611.
5. Ross R. Atherosclerosis–an inflammatory disease [Research Support, U.S. Gov't, P.H.S. Review]. N Engl J Med. 1999 Jan 14;340(2):115–126. PubMed PMID: 9887164; eng.
6. Tadros TM, Massaro JM, Rosito GA, Hoffmann U, Vasan RS, Larson MG, Keaney JF, Lipinska I, Meigs JB, Kathiresan S, et al. Pericardial fat volume correlates with inflammatory markers: the Framingham heart study [Research Support, N.I.H., Extramural Research Support, Non-U.S. Gov't]. Obesity (Silver Spring). 2010

May;18(5):1039–1045. PubMed PMID: 19875999; PubMed Central PMCID: PMC3014610. eng.
7. Leff T, Granneman JG, editors. Adipose tissue in health and disease. 1 ed. Federal Republic of Germany: Wiley-VCH Verlag GmbH & Co. KGaA, Weinheim; 2010.
8. Shields KJ, Stolz D, Watkins SC, Ahearn JM. Complement proteins C3 and C4 bind to collagen and elastin in the vascular wall: a potential role in vascular stiffness and atherosclerosis. Clin Transl Sci. 2011 Jun;4(3):146–152. PubMed PMID: 21707943; eng.
9. Santelices LC, Rutman SJ, Prantil-Baun R, Vorp DA, Ahearn JM. Relative contributions of age and atherosclerosis to vascular stiffness [Research Support, N.I.H., Extramural]. Clin Transl Sci. 2008 May;1(1):62–66. PubMed PMID: 20443820; eng.
10. Shields KJ, Barinas-Mitchell E, Gingo MR, Tepper P, Goodpaster BH, Kao AH, Manzi S, Sutton-Tyrrell K. Perivascular adipose tissue of the descending thoracic aorta is associated with systemic lupus erythematosus and vascular calcification in women [Research Support, N.I.H., Extramural]. Atherosclerosis. 2013 Nov;231(1):129–135. PubMed PMID: 24125423; PubMed Central PMCID: PMC3831349. eng.
11. Antonopoulos AS, Sanna F, Sabharwal N, Thomas S, Oikonomou EK, Herdman L, Margaritis M, Shirodaria C, Kampoli A-M, Akoumianakis I, et al. Detecting human coronary inflammation by imaging perivascular fat. Sci Transl Med. 2017 Jul 12;9(398):eaal2658. PubMed PMID: 28701474.
12. Alvey NJ, Pedley A, Rosenquist KJ, Massaro JM, O'Donnell CJ, Hoffmann U, Fox CS. Association of fat density with subclinical atherosclerosis [Research Support, N.I.H., Extramural]. J Am Heart Assoc. 2014 Aug;3(4). PubMed PMID: 25169793; PubMed Central PMCID: PMC4310364. eng. DOI:10.1161/JAHA.114.000788
13. Campbell GM, Sophocleous A. Quantitative analysis of bone and soft tissue by micro-computed tomography: applications to ex vivo and in vivo studies. Bonekey Rep. 2014;3:564. PubMed PMID: 25184037; PubMed Central PMCID: PMC4140449. eng.
14. Verdelis K, Szabo-Rogers HL, Xu Y, Chong R, Kang R, Cusack BJ, Jani P, Boskey AL, Qin C, Beniash E. Accelerated enamel mineralization in Dspp mutant mice. Matrix Biology. 2016 May-Jul;52-54:246–259. PubMed PMID: 26780724; PubMed Central PMCID: PMC4875851. eng.
15. Freeman TA, Patel P, Parvizi J, Antoci V, Shapiro IM. Micro-CT analysis with multiple thresholds allows detection of bone formation and resorption during ultrasound-treated fracture healing [Research Support, Non-U.S. Gov't]. J Orthop Res. 2009 May;27(5):673–679. PubMed PMID: 19016539; eng.
16. Suo J, Ferrara DE, Sorescu D, Guldberg RE, Taylor WR, Giddens DP. Hemodynamic shear stresses in mouse aortas: implications for atherogenesis [Research Support, N.I.H., Extramural Research Support, Non-U.S. Gov't]. Arterioscler Thromb Vasc Biol. 2007 Feb;27(2):346–351. PubMed PMID: 17122449; eng.
17. Langheinrich AC, Michniewicz A, Bohle RM, Ritman EL. Vasa vasorum neovascularization and lesion distribution among different vascular beds in ApoE-/-/LDL-/- double knockout mice [Research Support, N.I.H., Extramural Research Support, Non-U.S. Gov't]. Atherosclerosis. 2007 Mar;191(1):73–81. PubMed PMID: 16806224; eng.
18. Judex S, Luu YK, Ozcivici E, Adler B, Lublinsky S, Rubin CT. Quantification of adiposity in small rodents using micro-CT [Research Support, N.I.H., Extramural Research Support, U.S. Gov't, Non-P.H.S. Review]. Methods. 2010 Jan;50(1):14–19. PubMed PMID: 19523519; PubMed Central PMCID: PMC2818008. eng.
19. Pai VM, Kozlowski M, Donahue D, Miller E, Xiao X, Chen MY, Yu Z-X, Connelly P, Jeffries K, Wen H. Coronary artery wall imaging in mice using osmium tetroxide and micro-computed tomography (micro-CT) [Research Support, N.I.H., Extramural Research Support, N.I.H., Intramural Research Support, U.S. Gov't, Non-P.H.S.]. J Anat. 2012 May;220(5):514–524. PubMed PMID: 22360411; PubMed Central PMCID: PMC3323699. eng.
20. Ashton JR, Befera N, Clark D, Qi Y, Mao L, Rockman HA, Johnson GA, Badea CT. Anatomical and functional imaging of myocardial infarction in mice using micro-CT and eXIA 160 contrast agent. Contrast Media Mol Imaging. 2014 Mar-Apr;9(2):161–168. PubMed PMID: 24523061; PubMed Central PMCID: PMCPMC4017375.
21. Dunmore-Buyze PJ, Tate E, Xiang F-L, Detombe SA, Nong Z, Pickering JG, Drangova M. Three-dimensional imaging of the mouse heart and vasculature using micro-CT and whole-body perfusion of iodine or phosphotungstic acid [Research Support, Non-U.S. Gov't]. Contrast Media Mol Imaging. 2014 Sep-Oct;9(5):383–390. PubMed PMID: 24764151; eng.
22. Bouxsein ML, Boyd SK, Christiansen BA, Guldberg RE, Jepsen KJ, Müller R. Guidelines for assessment of bone microstructure in rodents using micro-computed tomography [Review]. J Bone Miner Res. 2010 Jul;25(7):1468–1486. PubMed PMID: 20533309; eng.
23. Zagorchev L, Oses P, Zhuang ZW, Moodie K, Mulligan-Kehoe M, Simons M, Couffinhal T. Micro computed tomography for vascular exploration. J Angiogenes Res. 2010;2:7. PubMed PMID: 20298533; PubMed Central PMCID: PMC2841094. eng.
24. Rajsheker S, Manka D, Blomkalns AL, Chatterjee TK, Stoll LL, Weintraub NL. Crosstalk between perivascular adipose tissue and blood vessels [Research Support, N.I.H., Extramural Review]. Curr Opin Pharmacol. 2010 Apr;10(2):191–196. PubMed PMID: 20060362; PubMed Central PMCID: PMC2843777. eng.
25. Trayhurn P, Wood IS. Signalling role of adipose tissue: adipokines and inflammation in obesity [Research Support, Non-U.S. Gov't Review]. Biochem Soc Trans. 2005 Nov;33(Pt 5):1078–1081. PubMed PMID: 16246049; eng.
26. Ohyama K, Matsumoto Y, Amamizu H, Uzuka H, Nishimiya K, Morosawa S, Hirano M, Watabe H, Funaki Y, Miyata S, et al. Association of coronary perivascular adipose tissue inflammation and drug-eluting stent-induced coronary hyperconstricting responses in pigs: 18F-fluorodeoxyglucose positron emission tomography imaging study. Arterioscler

Thromb Vasc Biol. 2017 Sep;37(9):1757–1764. PubMed PMID: 28751570.

27. Hofmann SM, Perez-Tilve D, Greer TM, Coburn BA, Grant E, Basford JE, Tschöp MH, Hui DY. Defective lipid delivery modulates glucose tolerance and metabolic response to diet in apolipoprotein E-deficient mice [Research Support, N.I.H., Extramural Research Support, Non-U.S. Gov't]. Diabetes. 2008 Jan;57(1):5–12. PubMed PMID: 17914034; PubMed Central PMCID: PMC2830804. eng.
28. Huang ZH, Reardon CA, Mazzone T. Endogenous ApoE expression modulates adipocyte triglyceride content and turnover [Research Support, N.I.H., Extramural Research Support, Non-U.S. Gov't]. Diabetes. 2006 Dec;55(12):3394–3402. PubMed PMID: 17130485; eng.
29. Tontonoz P, Hu E, Spiegelman BM. Stimulation of adipogenesis in fibroblasts by PPAR gamma 2, a lipid-activated transcription factor [Research Support, Non-U.S. Gov't Research Support, U.S. Gov't, P.H.S.]. Cell. 1994 Dec 30;79(7):1147–1156. PubMed PMID: 8001151; eng.
30. Henegar C, Tordjman J, Achard V, Lacasa D, Cremer I, Guerre-Millo M, Poitou C, Basdevant A, Stich V, Viguerie N, et al. Adipose tissue transcriptomic signature highlights the pathological relevance of extracellular matrix in human obesity. Genome Biol. 2008 Jan 21;9(1):R14. PubMed PMID: 18208606; PubMed Central PMCID: PMCPMC2395253.
31. Khan T, Muise ES, Iyengar P, Wang ZV, Chandalia M, Abate N, Zhang BB, Bonaldo P, Chua S, Scherer PE. Metabolic dysregulation and adipose tissue fibrosis: role of collagen VI [Research Support, N.I.H., Extramural Research Support, Non-U.S. Gov't]. Mol Cell Biol. 2009 Mar;29(6):1575–1591. PubMed PMID: 19114551; PubMed Central PMCID: PMC2648231. eng.
32. Mariman ECM, Wang P. Adipocyte extracellular matrix composition, dynamics and role in obesity. Cell Mol Life Sci. 2010 Apr;67(8):1277–1292. PubMed PMID: 20107860; PubMed Central PMCID: PMCPMC2839497.
33. Cypess AM, Lehman S, Williams G, Tal I, Rodman D, Goldfine AB, Kuo FC, Palmer EL, Tseng Y-H, Doria A, et al. Identification and importance of brown adipose tissue in adult humans [Research Support, N.I.H., Extramural Research Support, Non-U.S. Gov't]. N Engl J Med. 2009 Apr 9;360(15):1509–1517. PubMed PMID: 19357406; PubMed Central PMCID: PMC2859951. eng.
34. Shields KJ, El Khoudary SR, Ahearn JM, Manzi S. Association of aortic perivascular adipose tissue density with aortic calcification in women with systemic lupus erythematosus. Atherosclerosis. 2017 Jul;262:55–61. PubMed PMID: 28521185.
35. Paigen B, Morrow A, Holmes PA, Mitchell D, Williams RA. Quantitative assessment of atherosclerotic lesions in mice [Research Support, Non-U.S. Gov't Research Support, U.S. Gov't, P.H.S.]. Atherosclerosis. 1987 Dec;68(3):231–240. PubMed PMID: 3426656; eng.
36. Sloop GD, Perret RS, Brahney JS, Oalmann M. A description of two morphologic patterns of aortic fatty streaks, and a hypothesis of their pathogenesis [Research Support, U.S. Gov't, P.H.S.]. Atherosclerosis. 1998 Nov;141(1):153–160. PubMed PMID: 9863548; eng.
37. Davies PF, Civelek M, Fang Y, Fleming I. The atherosusceptible endothelium: endothelial phenotypes in complex haemodynamic shear stress regions in vivo. Cardiovasc Res. 2013 Jul 15;99(2):315–327. PubMed PMID: 23619421; PubMed Central PMCID: PMCPMC3695748.
38. Langheinrich AC, Michniewicz A, Sedding DG, Walker G, Beighley PE, Rau WS, Bohle RM, Ritman EL. Correlation of vasa vasorum neovascularization and plaque progression in aortas of apolipoprotein E(-/-)/low-density lipoprotein(-/-) double knockout mice [Research Support, N.I.H., Extramural Research Support, Non-U.S. Gov't]. Arterioscler Thromb Vasc Biol. 2006 Feb;26(2):347–352. PubMed PMID: 16293797; eng.